Seismicity associated with the 2004-2006 renewed ground uplift at campi flegrei caldera, Italy

G. Saccorotti, S. Petrosino, F. Bianco, M. Castellano, D. Galluzzo, M. La Rocca, E. del Pezzo, L. Zaccarelli, P. Cusano

Accepted Manuscript

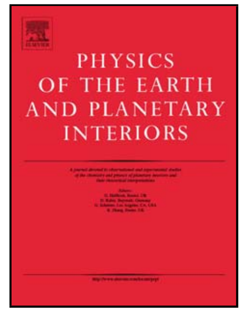

Title: Seismicity associated with the 2004-2006 renewed ground uplift at campi flegrei caldera, Italy

Authors: G. Saccorotti, S. Petrosino, F. Bianco, M. Castellano, D. Galluzzo, M. La Rocca, E. Del Pezzo, L. Zaccarelli, P. Cusano

PII:	S0031-9201(07)00149-5
DOI:	doi:10.1016/j.pepi.2007.07.006
Reference:	PEPI 4855
To appear in:	*Physics of the Earth and Planetary Interiors*
Received date:	20-3-2007
Revised date:	11-6-2007
Accepted date:	19-7-2007

Please cite this article as: Saccorotti, G., Petrosino, S., Bianco, F., Castellano, M., Galluzzo, D., La Rocca, M., Del Pezzo, E., Zaccarelli, L., Cusano, P., Seismicity associated with the 2004-2006 renewed ground uplift at campi flegrei caldera, Italy, *Physics of the Earth and Planetary Interiors* (2007), doi:10.1016/j.pepi.2007.07.006

SEISMICITY ASSOCIATED WITH THE 2004-2006 RENEWED GROUND UPLIFT AT CAMPI FLEGREI CALDERA, ITALY.

G. Saccorotti [1,], S. Petrosino[1], F. Bianco[1], M. Castellano[1], D. Galluzzo[1], M. La Rocca[1], E. Del Pezzo[1], L. Zaccarelli[1], P. Cusano[1]*

[1] Istituto Nazionale di Geofisica e Vulcanologia – Osservatorio Vesuviano
Via Diocleziano 328, 80124 Napoli (I)

(*)
Corresponding Author;
Now at Istituto Nazionale di Geofisica e Vulcanologia – Sez. di Pisa.
Via U. della Faggiola, 32 -56126 Pisa (I)
Tel. +39 050 8311960
Fax +39 050 8311942
e-mail saccorotti@pi.ingv.it

Submitted to

Physics of the Earth and Planetary Interiors
1st Revised Version of 11 June 2007

ABSTRACT

Following the significant ground uplift (~ 1.8 m) of the 1982-1984 bradyseismic crisis, the recent history of Campi Flegrei volcanic complex (Italy) has been dominated by a subsidence phase. Recent geodetic data demonstrate that the subsidence has terminated, and that positive ground deformation renewed in November 2004, at a low but accelerating rate leading to about 4 cm of uplift by the end of October, 2006. As in previous episodes, ground uplift has been accompanied by swarms of micro-earthquakes ($M \leq 1.4$) in three distinct episodes: ~~on~~ October 2005, October 2006 and December 2006. Hypocenters of these earthquakes are mainly located beneath the Solfatara Volcano at depths ranging between 0.5 and 4 km. Inversion of S-wave spectra indicates source radius and stress drop on the order of 30-60 m and $10^4 – 9 \times 10^5$ Pa, respectively. Fault plane solutions indicate predominantly normal mechanisms. Accompanying the October 2006 swarm, we detected intense Long-Period (LP) activity for about one week. These signals consist of weak, monochromatic oscillations whose spectra exhibit a main peak at frequency ~ 0.8 Hz. This peak is common to all the stations of the network, and not present in the noise spectra, suggesting that it is a source effect. About 75% of the detected LPs cluster into three groups of mutually similar events. Adjustment of waveforms using cross-correlation allows for precise alignment and stacking, which enhances signal onsets and permits accurate absolute arrival picks, and thus better absolute as well as relative locations. Locations associated with the three different clusters are very similar, and appear to delineate the SE rim of the Solfatara Volcano at a depth of about 500 m. The most likely source process for the LP events involves the resonance of a fluid-filled, buried cavity. Quality factors of the resonator cluster in a narrow interval around 4, which is consistent with the vibration of a buried cavity filled with a water-vapour mixture at poor gas-volume fractions. We propose a conceptual model to interpret the temporal and spatial patterns of the observed seismicity.

Key Words:
Volcano Seismology, Long Period Seismicity, Volcano Monitoring, Caldera, Hydrothermal System.

1. INTRODUCTION

Campi Flegrei (CF) volcanic complex is a nested caldera located in a densely populated area (~ 1.5 million inhabitants) west of Naples, Southern Italy. Its evolution has been characterized by many eruptive episodes, the most important of which are the large Campanian Ignimbrite (40ky b.p.; VEI=5) and the Neapolitan Yellow Tuff (15ky b.p.; VEI=6) eruptions (Scandone et al., 1991); its last activity occurred in 1538 AD, with the Monte Nuovo eruption (Di Vito et al., 1999). The most prominent feature of CF activity is the widely known phenomenon called "bradyseism", consisting of noticeable, fast ground uplifts followed by slow subsidence phases. The most recent bradyseismic crisis occurred in 1982-1984, during which a net uplift of 1.8 m centered on Pozzuoli town (Fig. 1) was accompanied by more than 16,000 earthquakes (M_{max} = 4.0) mostly located beneath the Pozzuoli-Solfatara area (Fig. 1), at depths between 0 and 4 km (Aster et al., 1992). These earthquakes were recorded by one of the first digital, mobile seismic networks, thus providing an invaluable data set that allowed a wide research community to investigate both the subsurface velocity structure and the dynamics of the seismic source (Vanorio et al., 2005, and references therein). Since January, 1985, the area has undergone a phase of general subsidence interspersed by minor, short-duration uplifts in 1989, 1994 and 2000. A characteristic of these movements is that seismicity always accompanies the uplift phases, while the subsidence occurs aseismically (Saccorotti et al., 2001). Of these minor uplift episodes, the one which began in March, 2000 constitutes a case of special interest. In July-August, 2000, ground deformation reached a maximum value of about 4 cm, and two swarms of low-magnitude earthquakes occurred over a period of three months. The first of these two swarms was mainly comprised of Long-period (LP) events, previously unobserved in Campi Flegrei seismicity (Saccorotti et al., 2001; Bianco et al., 2004). After August 2000, subsidence renewed; according to geodetic observation this phase stopped on November 2004 with the onset of a new uplift episode reaching a level of about 4 cm by the end of October, 2006 (Troise et al., 2007). This last phase shows an uplift rate lower than that of 2000, and the final ground deformation measurements indicate a general cessation of the phenomenon. Remarkable swarms of both Volcano-Tectonic (VT) and LP earthquakes have accompanied the ground uplift, with the highest number of seismic events ever recorded since 1985. This last unrest constitutes an event of high importance for both scientific and civil protection reasons, and has been monitored with great attention. This paper describes the seismological aspects of this phase, aiming at a detailed and quantitative description of the seismicity pattern, high precision location of the sources, focal mechanisms of VT events and the dynamic signature of the LP source. A conceptual model is then discussed to interpret the phenomenon in a unified framework including the most relevant geological and geophysical constraints.

2. SEISMICITY ACCOMPANYING THE 2005-2006 UNREST

2.1 Data

With the renewal of seismic activity, the permanent monitoring seismic network managed by Istituto Nazionale di Geofisica e Vulcanologia – Osservatorio Vesuviano (INGV – OV) was promptly complemented by a temporary deployment consisting of digital recorders, mostly equipped with broadband sensors, and a small-aperture array of short-period seismometers (Fig. 1). The overall deployment tracking the evolution of the 2005-2006 episode consisted of:

- 9 three-component short period analog stations;
- 1 three-component short period digital station;
- 8 three-component broadband (Lennartz LE-3D/20s, Guralp CMG40T 60 s) stations;
- 1 seismic antenna equipped with 5 three-components short period (Lennartz LE-3D/Lite 1Hz) sensors plus an accelerometer (Episensors Kinemetric).

This upgraded deployment significantly lowered the detection threshold of the permanent seismic network, doubling the number of locatable events and increasing the number of waveforms acquired with high Signal-to-Noise Ratio (SNR). All the instruments recorded in continuous mode, and detailed catalogs can be retrieved either by visual inspection or automatic picking procedures applied to the continuous data streams. Data presented in this paper include March 2005-December 2006; for consistency with previous determinations referred to the same area, magnitudes were retrieved from a duration-magnitude scale using data from station STH (Fig. 1).

2.2 Temporal evolution and signal classification

The quiet stage following the 2000 uplift episode ended on March 22, 2005, with the occurrence of a M= 0.4 event in the Solfatara -Accademia area (Fig. 1), at a depth of about 1.5 km. Following this event, visual inspection of the continuous data streams detected approximately 300 micro-earthquakes, most of which have very low magnitudes (M < 0; see Fig. 2). These signals exhibit waveform and spectral features that are indicative of a source process involving brittle shear failure, and are therefore classified as Volcano-Tectonic (VT) earthquakes (Fig. 3). This activity was concentrated within three distinct sequences. The first swarm occurred on October 5th 2005, and consisted of ~ 90 micro earthquakes (M_{max}=1.1). The second swarm occurred one year later, and consisted of approximately 160 micro earthquakes (M_{max}=0.8) from October 19-30, 2006. This activity was also accompanied by several hundreds of weak events characterized by lack of clear S-wave arrival, spindle-shaped waveforms and monochromatic low frequency spectra. We classified these signals as Long-Period (LP) events (Fig. 3). We created single-station LP bulletins using an automatic picking procedure based on detection of peak values of the three-component envelope of the 0.5-2 Hz band-pass filtered continuous data streams from a selected number of stations. A final catalogue was derived by applying a trigger coincidence criterion to data from stations ASB2 and AMS2, which depicted the best SNR. This final catalogue includes 338 events occurred during the October 20-30, 2006, time interval (Fig. 2). LP activity climaxed on October 27, 2007, about 1 day after the period of most intense VT activity. The last VT swarm occurred on December 21, 2006, with 8 earthquakes having the highest magnitude (M_{max}=1.4) of the entire period (Fig. 2).

2.3 Location and Source parameters of VT events

We evaluated the locations of the recorded VT seismicity by inverting P- and S-wave arrival times following the probabilistic grid search approach of Tarantola and Vallette (Tarantola and Vallette, 1982). The search for the minimum-misfit solution is conducted using the Metropolis–Gibbs algorithm (Lomax et al., 2000). Theoretical travel times at the different stations are obtained in a 3D velocity structure derived from a recent tomographic experiment (Judenherc and Zollo, 2004). Results are reported in Figure 4, which shows the spatial distribution of the cumulative, marginal probability density associated with 83 events. Most of the seismicity is clustered at depths between 1 and 4 km. Closer examination of the temporal evolution of hypocentral data indicates that the first two swarms (October 2005; October 2006) have very similar locations, being clustered beneath the Solfatara Volcano at depths of 1.5-2.5 km. Conversely, earthquakes from the December 2006 swarm are located some 2 km to the north, at depths of 0-2 km beneath the Astroni Crater (Fig. 4). As illustrated in Figure 3, the spectral signature of this seismicity is typical of earthquakes generated through brittle shear failure processes, with corner frequencies in the range 10 – 16 Hz. Using data from station STH, located close to the Solfatara area (Fig. 1), we calculate the seismic moment, the source radius and the stress drop associated with VT seismicity. For this procedure, we first obtained displacement S-wave spectra by log-averaging the smoothed spectra of the EW and NS components calculated over a 2.5 s time window starting at the S-wave arrival. We thus fitted the spectra to the theoretical Brune's source model using S-wave velocity of 1.5 km/s, Qs=110 (Del Pezzo et al., 1987), and a density of 2200 kg/m^3. Results indicate source radii in the range 30 – 60 m, stress drop in the range 10^4 – 9 x 10^5 Pa, and Seismic Moment in the range 10^9- 10^{11} J for events with Magnitude in the range -0.5 / 1.4. Source dimensions, stress-drop and Moments are of the same order of those observed during the 1982-84 seismic swarm and the 2000 crisis (stress drops generally lower than 1 MPa and source dimensions on the order of 100 m), suggesting that the present sequence shares the same mechanism of these two previous episodes (Saccorotti et al., 2001). Assuming a double couple mechanism, we then calculated fault plane solutions applying the grid-search algorithm FPFIT (Reasemberg and Oppenheimer, 1985) to the P-wave first motion polarities for a selected subset of the best-located events. From the whole data set, we selected 10 earthquakes (0.40≤ M ≤1.40) with at least eight reliable P-onset polarity readings. The resulting focal mechanisms are reported in Figure 5. A class of normal solutions may be recognized with nodal planes rotating from N-S toward NNE–SSW and finally to NNW–SSE. The events belonging to the October 2006 swarm, (that exhibit very similar waveforms), show very similar fault plane solutions; the same observation is valid for the events belonging to the December 2006 swarm as well.

2.4 LP Activity

LP signals occurring during the October 20-30, 2006 swarm consist of spindle-shaped, monochromatic oscillations, whose spectra are typically peaked at frequencies between 0.7-1 Hz (Fig. 3). Several factors, such as: (a) the absence of this peak in either the noise or earthquake spectra, and (b) the persistence of this peak among all the stations of the network, suggest that it reflects a source effect (Figs. 3 and 6). The weakness of these signals, and their emergent onsets, make impossible the application of any location procedure based on inversion of P-wave arrival times. However, once band-pass filtered around the main frequency peak, the LP signals share a common signature. We quantified this observation by conducting correlation analyses for all the independent event pairs using 15-second windows encompassing the preliminary time pickings for the radial-component recordings of stations ASB2, AMS2, BGNG, OMN2. Eventually, we averaged these matrices in order to obtain a single, network-representative similarity matrix. Application of a sequential, exclusive clustering procedure allowed identifying three clusters of events for which the similarity among all the independent member pairs was greater than or equal to 0.6. For each group of similar events, we used the preliminary time picks and the precise, inter-event time delays derived from correlation analyses to obtain consistent alignment of waveforms (e.g., Shearer, 1997). A complete description of the procedure is found in Saccorotti et al. (2007).

Since the number of differential time estimates is generally much larger than that of the preliminary time picks, the arrival times derived from the above procedure provide a consistent alignment of waveforms, but the signal onsets are not necessarily correct. As a last step, therefore, we derived absolute time picks by correcting the adjusted arrival times for the visually-estimated onset of the stacked waveforms (Rowe et al., 2004) (Fig. 7). For the location procedure, we used the same nonlinear probabilistic inversion previously adopted for VT signals. For each cluster, we first located the stacked event, and then used the residuals from this location as station terms for the subsequent location of the cluster members. In this manner, the systematic errors due to incomplete knowledge of the earth structure are eliminated, while high precision in the relative positions of individual hypocenters is ensured by the previously-obtained least-square adjustment of first arrivals. The three different clusters depict very similar locations, and appear to delineate the SE rim of the Solfatara crater at a depth of about 500 m (Fig. 8). The proximity of the three clusters is in agreement with the similarity of the respective stacked waveforms (Fig. 9). The monochromatic character of LP oscillations (Figs. 3 and 6) suggests that these signals are generated by a resonance process. The marked waveform similarity persisting throughout the analysed time interval indicates the involvement of a non-destructive source process. Taken together, these observations suggest that the LP-generating process most likely represents the harmonic oscillation of a fluid-filled reservoir repeatedly triggered by time-localized pressure steps (e.g., Crosson and Bame, 1985; Chouet, 1988, 1996; Fujita et al., 1995; Jousset et al., 2003; Neuberg et al., 2000). Following this hypothesis, the quality factor and dominant frequency of the resonator may provide hints about the composition and physical properties of the fluid contained in the cavity. Using LP power spectral estimates, we measure the quality factor Q of the resonator from the relationship:

$$Q = f / \Delta f \qquad (1)$$

where f is the frequency corresponding to a dominant spectral peak and Δf is the width of that peak at half the peak's magnitude. We applied eq. (1) to the radial component of motion for the set of located events at stations ASB2 (Fig. 10). In both cases, distributions of Q are peaked at values around 4. This value is significantly smaller than those observed at other volcanoes. Q estimates from the literature span ~~in fact~~ the 10-500 range, the lower and upper bounds being associated with LPs observed at Kilauea volcano, Hawaii (Kumagai et al., 2005) and Galeras volcano, Colombia (Kumagai and Chouet, 1999). The quality factor is composed by two terms:

$$Q^{-1} = Q_i^{-1} + Q_r^{-1}, \qquad (2)$$

where Q_i^{-1} expresses the intrinsic attenuation in the fluid and Q_r^{-1} refers to energy losses at the fluid-rock interface.

While Q_i only depends on the physical properties of the fluid, Q_r is a function of both the impedance contrast at the fluid-rock interface and the geometry of the resonating cavity. The different models thus far proposed for the source of LP events account for cylindrical (e.g., Chouet, 1985), spherical (Crosson and Bame, 1985; Fujita, 1995; Fujita and Ida, 1999), or crack-like (Chouet, 1986; 1988) geometries. In particular, Chouet's studies demonstrated the existence of a very slow wave developing at the fluid-rock interface of the fluid-filled crack. This wave, named the crack wave, leads to more realistic estimates of the size and volume of a fluid-filled resonator as compared to a resonator with spherical geometry. Moreover, the crack geometry is also appropriate to satisfy mass transport conditions beneath volcanoes. Based on these considerations, we assume that the source of our LP signals has a crack-like geometry.

The acoustic properties of a fluid-filled fracture under a variety of fluid and rock-matrix properties were investigated in detail by Kumagai and Chouet (1999; 2000), who later examined (Kumagai and Chouet, 2001) the dependence of such properties on the crack geometry and vibration modes.

These studies demonstrated that the wide range spanned by Q measurements may be explained in terms of the different physical properties of the multiphase fluid mixtures and the surrounding rock matrix. Although Kumagai and Chouet's results demonstrated that the association between a given Q value and the composition and physical properties of the fluid may be manifold, their conclusions indicate that the high decay rate observed for our LP events can only be explained in terms of a very low impedance contrast at the fluid-rock interface, which prevents the trapping of elastic energy inside the fissure. Several multiphase mixtures may fulfil such a condition (see Plate 1 in Kumagai and Chouet, 2000, and Fig. 1 in Kumagai and Chouet, 2001); however, the absence of any surface-visible phenomena and the shallow depth of the LP source volume indicate that the most likely candidate for the LP-generating process is the vibration of a fracture filled with a water-vapour mixture at low gas-volume fractions. For instance, a fracture filled by bubbly water at 1-1.5% gas-volume fraction would exhibit Q_r^{-1} and Q_i^{-1} spanning the 0.2-1 and 0.05-0.001 ranges, respectively, thus resulting in a Q between 1 and 5. We obtained more resolved estimates of f and Q from Auto-Regressive modelling of the signal (The SOMPI method of Kumazawa et al., 1990). In agreement with the previous observations, these last results indicate $f \sim 0.7$ Hz ad $Q \sim 5\text{-}10$. Taken together, these results suggest that the LP activity is associated with the repeated pressurisation of water-filled fractures pertaining to the Solfatara hydrothermal system, which is expected to extend over the 0-1500 m depth range (Todesco et al., 2004), thus fully encompassing the hypocentral depths of our LP data.

3. DISCUSSIONS AND CONCLUSIONS

The seismic activity during the ongoing unrest episode at Campi Flegrei exhibits the following features:

- VT activity begins with the increase in the velocity of the ground uplift (see Fig. 2);
- With the exception of the December, 2006 swarm, most of the VT seismicity is confined beneath the Solfatara Volcano, at depths between 1 and 4 km;
- Focal mechanisms indicate a dominance of normal faults, indicative of a tensile stress regime;
- Source parameters and focal volumes are similar to those observed during the previous unrest episodes (Del Pezzo et al., 1987; Aster et al., 1992; Saccorotti et al., 2001), suggesting that these different awakening events are driven by a common dynamic;
- Most of the LP activity occurs after a step in the VT energy release, suggesting a possible cause-effect relationship between the two phenomena;
- The best located LP events cluster at a depth of about 500 m beneath the Solfatara Volcano, thus overlying the VT source region;
- The quality factor of the LP waveforms is consistent with the resonant vibration of a buried cavity filled with bubbly-water.

In a recent paper, Battaglia et al. (2006) used joint inversion of gravity and deformation data to propose a model of ground uplift and following subsidence for the major 1983-1984 bradyseismic crisis. According to these authors, the best fitting source for the initial uplift phase is the inflation of a penny-shaped, horizontal crack with density 142-1115 kg m^{-3} located at depths of 3-4 km beneath the centre of Pozzuoli (Fig. 1). Conversely, the late stages (1990-1995) of the subsidence phase are best represented by the deflation of an overlying, vertical spheroid source with a density of about 1000 kg m^{-3} and extending over the 1.5-2.5 km depth range. Based on these results, Battaglia et al. (2006) postulate that the whole deformation cycle (rapid inflation and subsequent, slow subsidence) may be explained in terms of fluid exchange between the deeper and the shallower reservoir. A critical point of this model is the existence of an impermeable level separating the two reservoirs. This sealed level would permit, at least in the early stages of the unrest, the pressurisation and consequent inflation of the deeper reservoir. In a subsequent paper, Troise et al. (2007) used vertical and horizontal ground deformation data to demonstrate that the most recent uplift episodes (including the present one) most likely represent the action of the same dynamic processes. Considering these points, the present unrest may be interpreted as due to overpressure within a cavity located at a depth of 3-4 km or more, and containing fluids of magmatic origin, such as volatiles and brines accumulating at the top of a degassing magma chamber. To explain the origin of this overpressure one may invoke the arrival of a batch of fresh, gas-rich magma from a deepseated source. In addition to ground deformation, the pressurization of this reservoir would also induce brittle failure in the overlying, rigid layer which, as suggested by the depth distribution of VT seismicity (Fig. 4), most likely extends over the 1 – 3 km depth range. During the October 2006 swarm, there must have been a critical level of fracturing which ~~has~~ permitted significant fluid leakage from the deeper reservoir toward the shallow hydrothermal system. As a consequence, some portion of the fracture network pertaining to the Solfatara hydrothermal system might have been subjected to rapid pressurization episodes which triggered its resonant, LP vibration (Fig. 11). In agreement with Battaglia et al. (2006) conclusions, our conceptual model suggests that the postulated magma intrusions occur at the very early stage of the unrest episode, thus preceding by a variable time interval the appearance of the most identifiable signals (e.g. ground deformation, earthquake swarms). In particular, LP activity most likely reflects the response of a shallow hydrothermal system to the heating and pressurisation caused by upward migration of magmatic fluids. These factors point to a double role played by hydrothermal systems beneath volcanoes. By inducing large ground deformations and sustained LP seismicity, these systems provide an amplified response to the arrival of fresh magmatic fluids. Such easily observed signals occur after the intrusion process itself, however, and their significance as a precursory tool is therefore highly questionable. Thus the need remains for reliable and detailed monitoring procedures able to detect subtle variations over a broad frequency interval. Hopefully, extensive deployments including borehole strain-meters, broad-band seismometers and tiltmeters will allow the detection and quantitative analysis of the weak geophysical signals associated with the very early stages of unrest episodes.

ACKNOWLEDGEMENTS

Thoughtful comments from Charlotte Rowe and an anonymous reviewer greatly helped to improve the quality of the manuscript. Work financed through the INGV-DPC projects and the European Commission, 6th Framework Project – 'VOLUME', Contract No. 08471.

REFERENCES

Aster, R.C., R.P. Meyer, G. De Natale, A. Zollo, M. Martini, E. Del Pezzo, R. Scarpa, G. Iannaccone, Seismic investigation of Campi Flegrei Caldera, In: Volcanic Seismology, Proc. Volcanol. Series III., 1992, Springer Verlag, New York.

Battaglia, M., C. Troise, F. Obrizzo, F. Pingue, G. De Natale, Evidence of fluid migration as the source of deformation at Campi Flegrei caldera (Italy), Geophys. Res. Lett. 33 (2006) L01307, doi:10.1029/2005GL024904.

Bianco, F., E. Del Pezzo, G. Saccorotti, G. Ventura, The role of hydrotermal fluids in triggering the july-august 2000 seismic swarm at Campi Flegrei (Italy): evidences from seismological and mesostructural data, J. Volcanol. Geoth. Res. 133 (2004) 229 – 246.

Chouet, B.A., Long Period volcano seismicity: its source and use in eruption forecasting, Nature 380 (1996) 309-316.

Chouet, B.A., Resonance of a fluid-driven crack: radiation properties and implications for the source of long-period events and harmonic tremor, J. Geophys. Res. 93 (1988) 4375–4400.

Crosson, R.S., D.A. Bame, A spherical source model for low frequency volcanic earthquakes, J. Geophys. Res. B. 90 (1985) 10237-10247.

Del Pezzo, E., G. De Natale, M. Martini, A. Zollo, Source parameters of microearthquakes at Phlaegrean Fields (Southern Italy) volcanic area, Phys. Earth Plan. Int. 47 (1987) 25-42.

Di Vito, M.A., R. Isaia, G. Orsi, J. Southon, S. de Vita, M. D'Antonio, L. Pappalardo, M. Piochi, Volcanism and deformation since 12,000 years at the Campi Flegrei caldera (Italy), J. Volcanol. Geoth. Res., 91 (1999) 221-246.

Fujita, E., Y. Ida, J. Oikawa, Eigen oscillation of a fluid sphere and source mechanism of harmonic volcanic tremor, J. Volcanol. Geoth. Res. 69 (1995) 365–378.

Fujita, E. and Ida, Y., Low attenuation resonance of a spherical magma chamber: Source mechanism of volcanic tremor at Asama volcano, Japan , Geophys. Res. Lett., 26 (1999) 3221-3224.

Jousset, P., J. Neuberg, S. Sturton, Modelling the time-dependent frequency content of low-frequency volcanic earthquakes, J. Volcanol. Geoth. Res. 128 (2003) 201–223.

Judenherc, S., A. Zollo, The Bay of Naples (southern Italy): Constraints on the volcanic structures inferred from a dense seismic survey, Geophys. Res. Lett. 109 (2004) B10312, doi:10.1029/2003JB002876.

Kumagai, H., B.A. Chouet, Acoustic properties of a crack containing magmatic or hydrothermal fluids, J. Geophys. Res. 105 (2000) 25493–25512.

Kumagai, H., B.A. Chouet, P.B. Dawson, Source process of a long period event at Kilauea volcano, Hawaii, Geophys. J. Int. 161 (2005) 243–254.

Kumagai, H., B.A. Chouet, The complex frequencies of long-period seismic events as probes of fluid composition beneath volcanoes, Geophys. J. Int. 138 (1999) F7–F12.

Kumagai, H., B.A. Chouet, The dependence of acoustic properties of a crack on the resonance mode and geometry, Geophys. Res. Lett. 28 (2001) 3325–3328.

Kumazawa, M., Y. Imanishi, Y. Fukao, M. Furumoto, Y. Yamamoto, A theory of spectral analysis based on the characteristic property of a linear dynamic system, Geophys. J. Int. 101 (1990) 613–630.

Lomax, A., J. Virieux, P. Volant, C. Berge, Probabilistic earthquake location in 3D and layered models: Introduction of a Metropolis-Gibbs method and comparison with linear locations, in: C.H. Thurber, N. Rabinowitz (Eds.), Advances in Seismic Event Location Kluwer , Amsterdam, 2000, pp. 101-134.

Neuberg, J., R. Luckett, B. Baptie, K. Olsen, Models of tremor and low-frequency earthquake swarms on Montserrat, J. Volcanol. Geoth. Res. 101 (2000) 83-104.

Reasemberg, P., D. Oppenheimer, FPFIT, FPPLOT and FPPAGE: Fortran computer programs for calculating and displaying earthquake fault-plane solutions, U.S. Geol. Surv. Open File Rep. (1985) 739, 109.

Rowe, C.A., C.H. Thurber, R.A. White, Dome growth behavior at Soufriere Hills Volcano, Montserrat, revealed by relocation of volcanic event swarms, 1995–1996. J. Volcanol. Geotherm. Res. 134 (2004) 199–221.

Saccorotti, G., F. Bianco, M. Castellano, E. Del Pezzo, The July-August 2000 seismic swarms at Campi Flegrei volcanic complex, Italy, Geophys. Res. Lett. 28 (2001) 2525 – 2528.

Saccorotti, G., I. Lokmer, C.J.Bean, G. Di Grazia and D. Patanè, Analysis of sustained long-period activity at Etna Volcano, Italy, J. Volcanol. Geotherm. Res. 160 (2007) 340-354.

Scandone, R., F. Bellucci, L. Lirer, G. Rolandi, The structure of the Campanian Plain and the activity of Neapolitan volcanoes, J. Volcanol. Geoth. Res., 48 (1991) 1-31.

Shearer, P.M. , Improving local earthquake locations using the L1-norm and waveform cross-correlation: application to the Whittier Narrows, California, aftershock sequence, J. Geophys. Res. 102 (1997) 8269–8283.

Tarantola, A., B. Vallette, Inverse problem = quest for information, J. Geophys. 50 (1982) 159–170.

Todesco, M., J. Rutqvist, G. Chiodini, K. Pruess, C.M. Oldenburg, Modeling of recent volcanic episodes at Phlegran Fields (Italy): geochemical variations and ground deformation, Geothermics, 33 (2004) 531-547.

Troise, C., G. De Natale, F. Pingue, F. Obrizzo, P. De Martino, U. Tammaro, Boschi E., Renewed ground uplift at Campi Flegrei caldera (Italy): New insight on magmatic processes and forecast, Geophys. Res. Lett. 34 (2007) L03301, doi:10.1029/2006GL028545.

Vanorio, T., J. Virieux, P. Capuano, G. Russo, Three-dimensional seismic tomography from P wave and S wave microearthquake travel times and rock physics characterization of the Campi Flegrei Caldera, J. Geophys. Res., 110 (2005) B03201, doi:10.1029/2004JB003102.

FIGURE CAPTIONS

Fig. 1 - Map of Campi Flegrei with the locations of the INGV - OV seismic network. Blue and yellow symbols refer to stations from the permanent and temporary network, respectively. We use circles for stations equipped with short period sensors, and triangles for stations equipped with broad-band sensors. ADM (the circle with the black point inside) is the site of the array (see text for details).

Fig. 2 – *a)* Monthly number of VT earthquakes and associated energy release, compared to the vertical ground deformation in Pozzuoli from continuous GPS measurements (redrawn from Troise et al., 2007). Energy is in units of 10^{10} J, and deformation (magnified 5 times) is in mm. *b)* Plot of the number of LP and VT earthquakes over 6-hour-long intervals during the October 20-30, 2006, time interval.

Fig. 3 – From top to bottom: Velocity seismograms, spectrograms and normalized displacement spectra for two events classified as (*a*) Volcano-Tectonic and (*b*) Long-Period ~~(left and right column, respectively)~~. Data are from the NS component of station ASB2 (see Fig. 1). Spectrograms are calculated using a 5.12-s-long window sliding along the seismograms with 75% overlap. Displacement spectra are obtained over a window of the same length encompassing the maximum peak-to-peak amplitude of ground velocity. The two events are essentially co-located beneath the Solfatara Volcano at a depth of about 500 m b.s.l..

Fig. 4 - Cumulative, marginal probability distributions of source locations (number of earthquakes/km^2) associated with the (*a*) horizontal plane and the two vertical planes oriented (*b*) NS and (*c*) EW. The maps have been obtained after stacking probability distributions retrieved from locations of individual earthquakes. The maximum-likelihood hypocenters associated with the October 2005, October 2006 and December 2006 swarms are drawn with black, white and grey dots, respectively.

Fig 5 - Fault plane solutions (lower hemisphere, equal area projection) for the ten events exhibiting the largest number of reliable P-wave polarity readings. Open and solid circles denote the dilatational and compressional P-wave first motion, respectively. P and T axes are also shown.

Fig. 6– (*a*) Radial-component velocity seismograms at all the stations of the broad-band network

for a sample LP event occurred on October 26, 2006, at 04:14:05 UT. Traces are arranged in order of increasing distance from the source. (*b*) Normalised power spectral estimates for the LP event and for 1-hour-long section of background noise (continuous and dashed lines, respectively). Noise spectra are dominated by a peak at frequency around 0.3 Hz, due to marine microseisms, and lack the LP distinctive peak at frequency around 0.8 Hz.

Fig. 7 – (*a*) Radial (NS) component of ground velocity at station ASB2 for 193 events pertaining to cluster n. 1. Traces are aligned to the automatic time pickings, 10 seconds into the recordings. (*b*) The same traces after the least-square adjustment of arrival times. (*c*) Stacked trace, and corresponding visual estimate of the signal's onset (vertical bold line).

Fig. 8– Maximum likelihood locations for the three different clusters superimposed to a shaded relief map of Solfatara Volcano and surroundings. We only show solutions with RMS residuals lower than 0.1 s, amounting to 132 events (more than 50% of the located events). Panels (*a*, *b* and *c*) as in Figure 4.

Fig. 9 – Stacked velocity seismograms for the three clusters of similar LP events. Data are from the NS (radial) component of station ASB2. The three stacked traces are individually normalised to their maximum peak-to-peak amplitude; their marked similarity is in agreement with the proximity of the respective source regions (Fig. 8).

Fig. 10 – Estimates of (*a*) quality factor Q and (*b*) dominant frequency f for the entire set of clustered LP events. Data are from the radial component of station ASB2; different grey tones correspond to data from the different clusters, using the same colour coding adopted in Fig. 8.

Fig. 11 –Proposed scenario for the seismicity accompanying the last unrest episode at Campi Flegrei. Accumulation of magmatic fluids (brine / gas) induces pressurization of a reservoir located at depths of 3-4 km, in turn providing the driving force for the onset of ground deformation. An overlying, rigid and impermeable layer begins fracturing, as suggested by the marked clustering of VT seismicity (stars) over the 1-3 km depth range. Upon reaching a critical fracturing level, fluids begin migrating from the deeper reservoir toward the shallower hydrothermal system, thus inducing rapid pressurization steps which trigger the LP vibrations of fractures filled by a water-steam mixture. Black dots mark LP hypocenters.

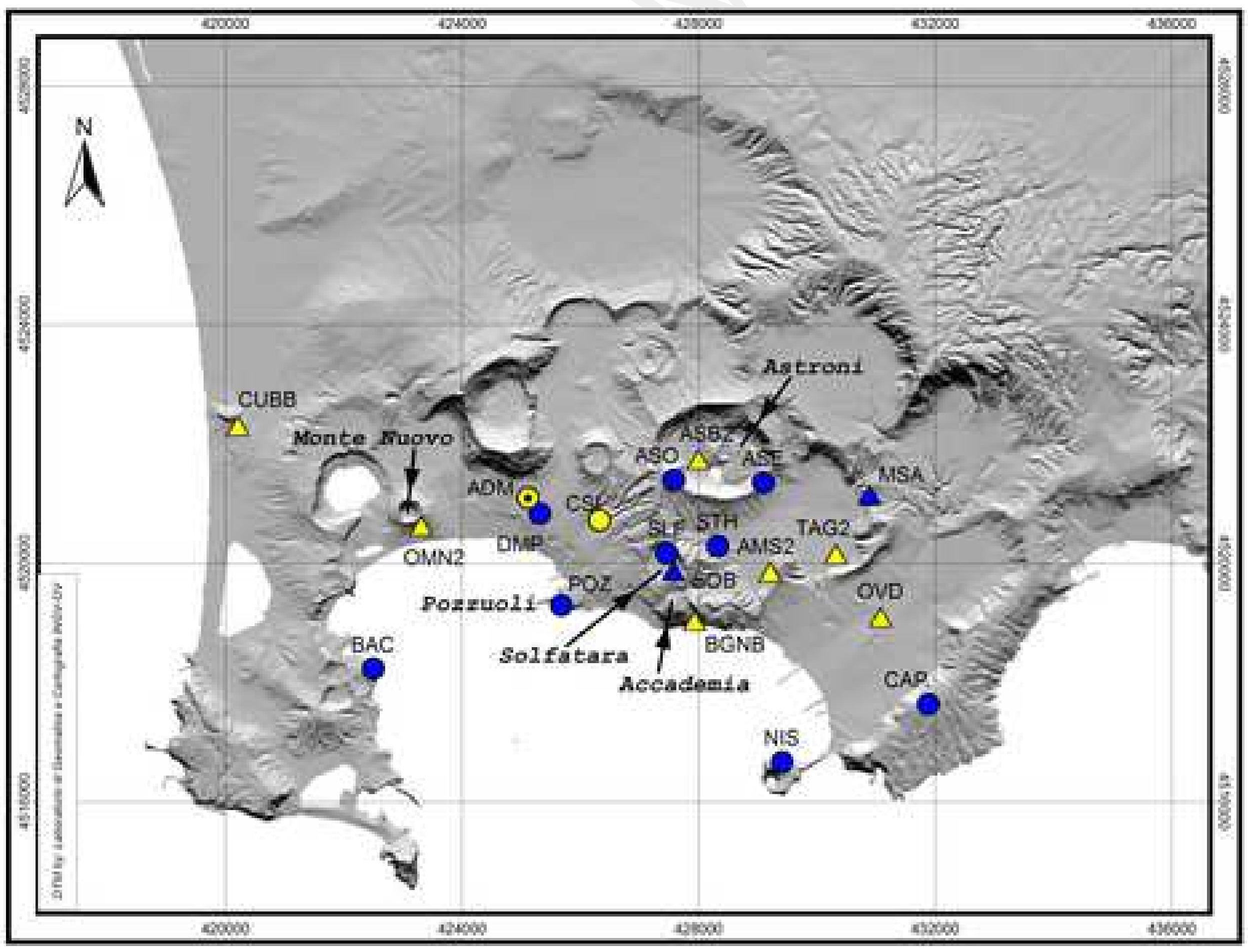
420000
424000
428000
432000
436000
N
CUBB
Monte Nuovo
OMN2
ADM
DMP
CSO
ASO
ASBZ
Astroni
ASE
MSA
SLF
STH
AMS2
TAG2
SOB
POZ
Pozzuoli
OVD
BGNB
Solfatara
Accademia
BAC
CAP
NIS

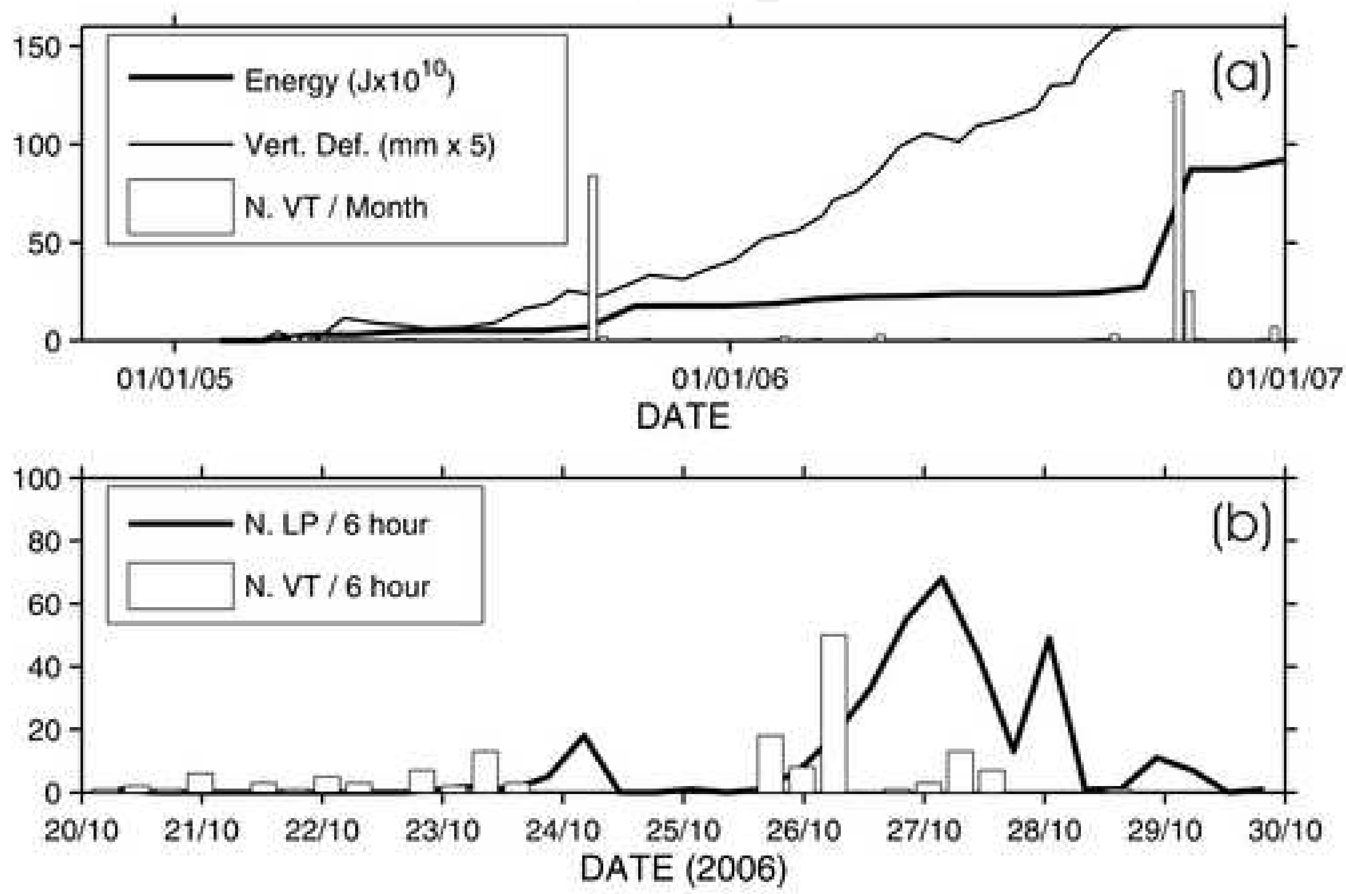

150
100
50
0
Energy (Jx10^10)
Vert. Def. (mm x 5)
N. VT / Month
(a)
01/01/05
01/01/06
01/01/07
DATE
100
80
60
40
20
0
N. LP / 6 hour
N. VT / 6 hour
(b)
20/10
21/10
22/10
23/10
24/10
25/10
26/10
27/10
28/10
29/10
30/10
DATE (2006)

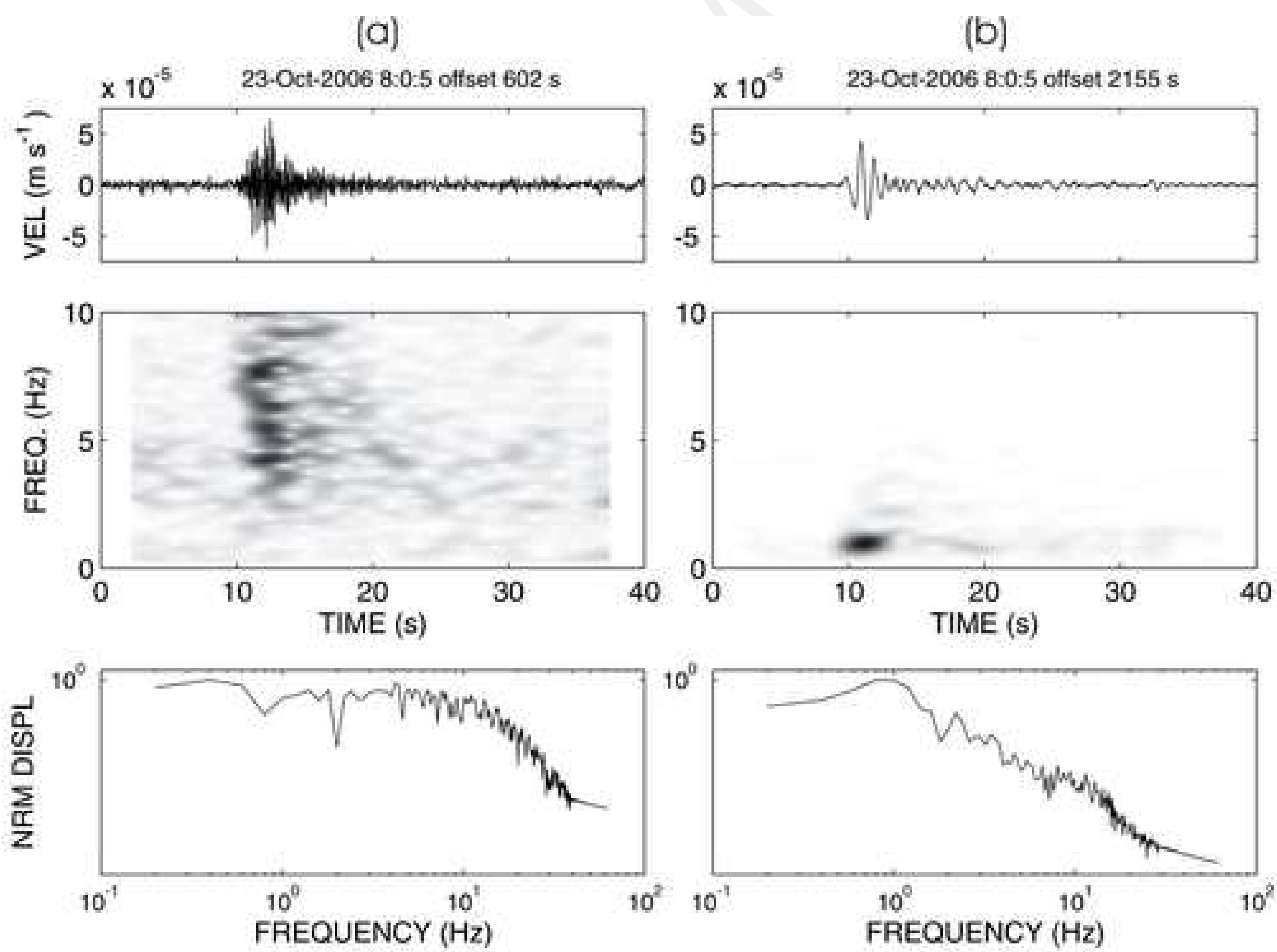

(a)
(b)
23-Oct-2006 8:0:5 offset 602 s
23-Oct-2006 8:0:5 offset 2155 s
x 10^-5
VEL (m s^-1)
FREQ. (Hz)
TIME (s)
NRM DISPL
FREQUENCY (Hz)

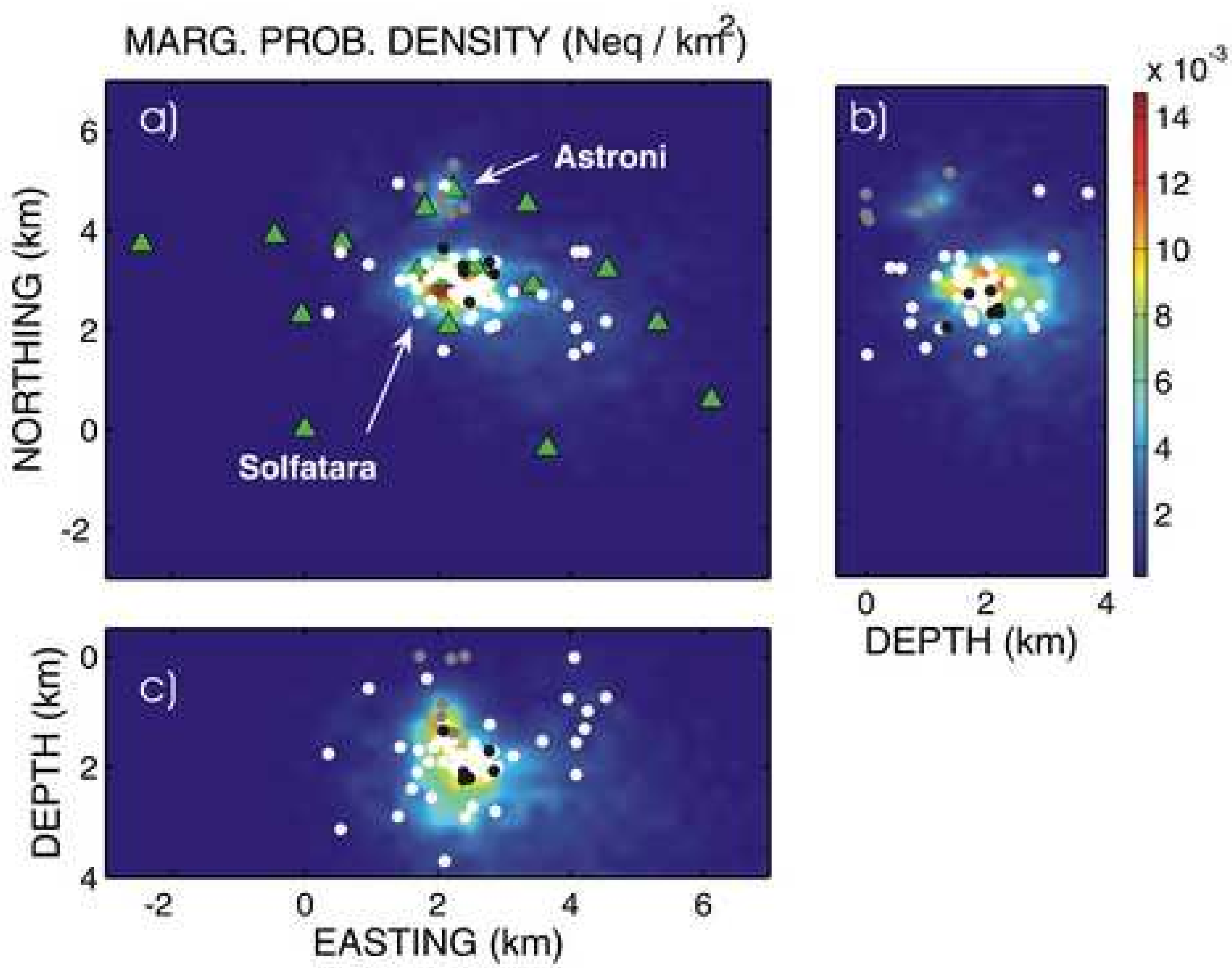
MARG. PROB. DENSITY (Neq / km^2)
a)
Astroni
Solfatara
NORTHING (km)
b)
DEPTH (km)
x 10^{-3}
c)
DEPTH (km)
EASTING (km)

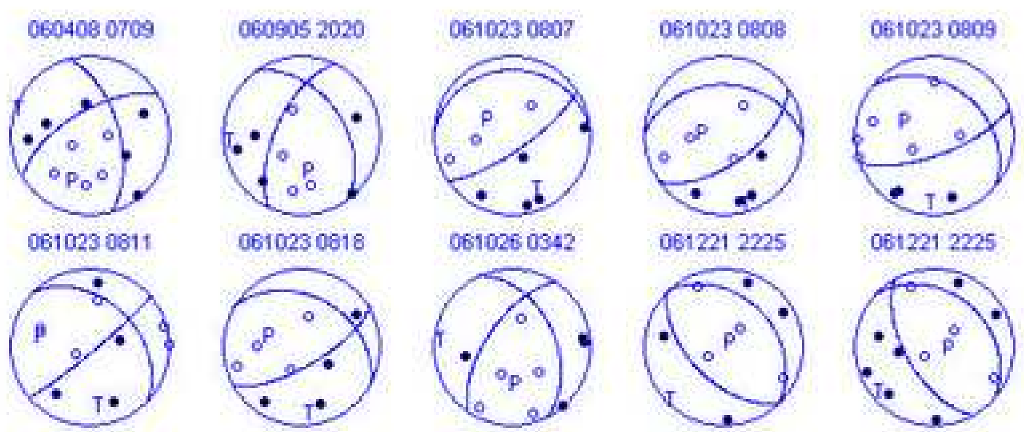
060408 0709
060905 2020
061023 0807
061023 0808
061023 0809
061023 0811
061023 0818
061026 0342
061221 2225
061221 2225

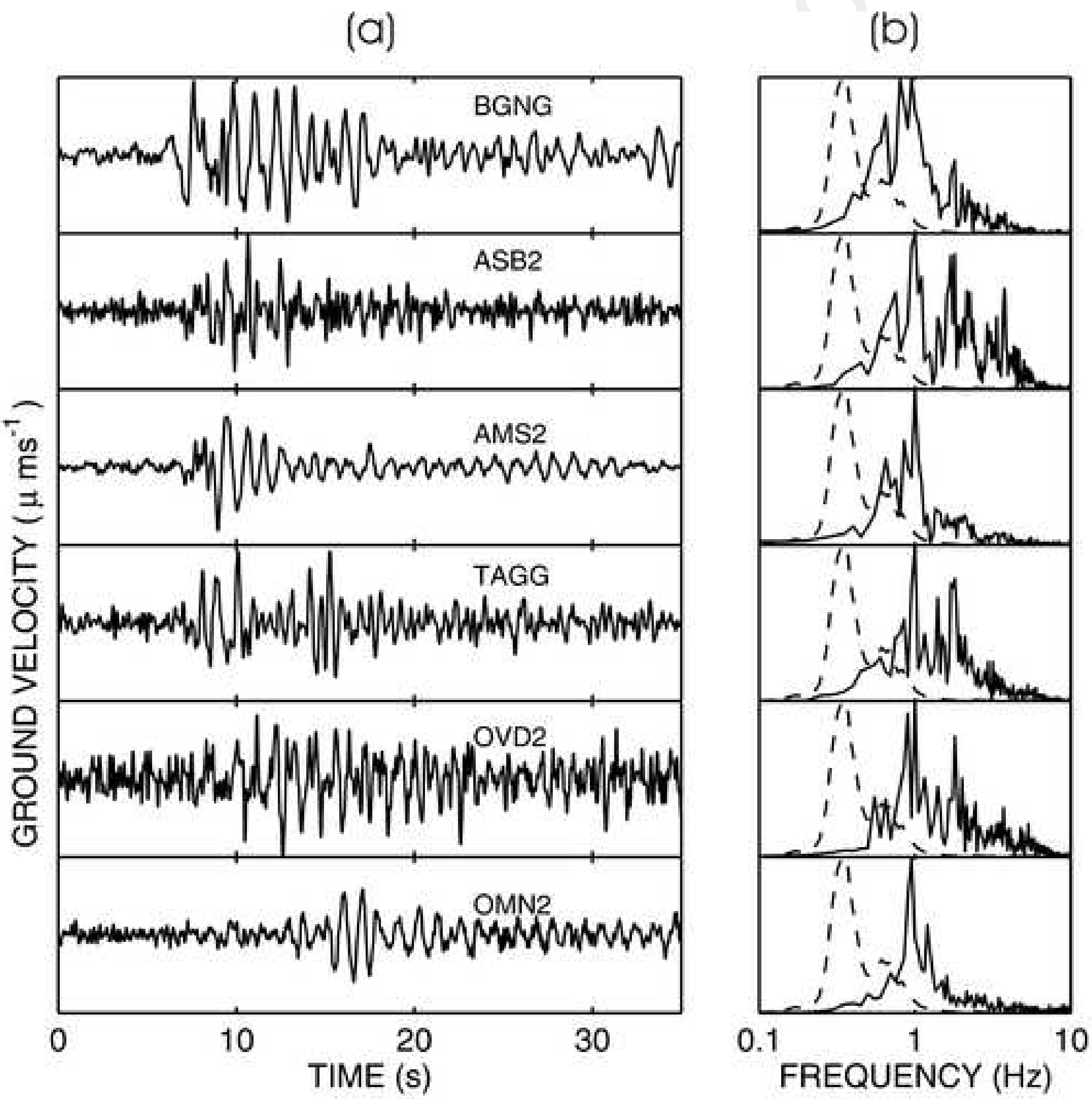
(a)
(b)
BGNG
ASB2
AMS2
TAGG
OVD2
OMN2
GROUND VELOCITY (μ ms^{-1})
0
10
20
30
TIME (s)
0.1
1
10
FREQUENCY (Hz)

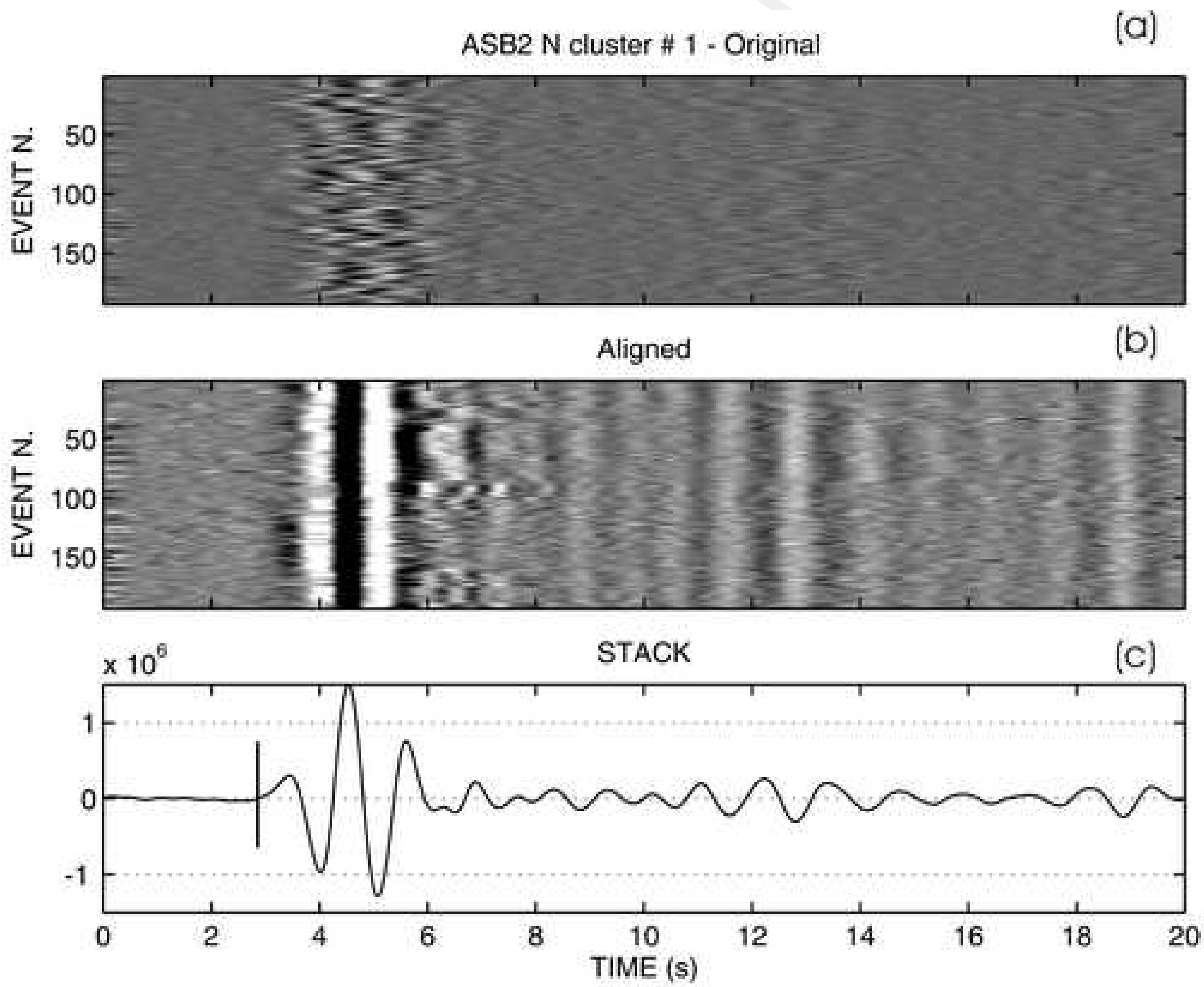

(a)
ASB2 N cluster # 1 - Original
EVENT N.
50
100
150
(b)
Aligned
EVENT N.
50
100
150
(c)
STACK
x 10^6
1
0
-1
0
2
4
6
8
10
12
14
16
18
20
TIME (s)

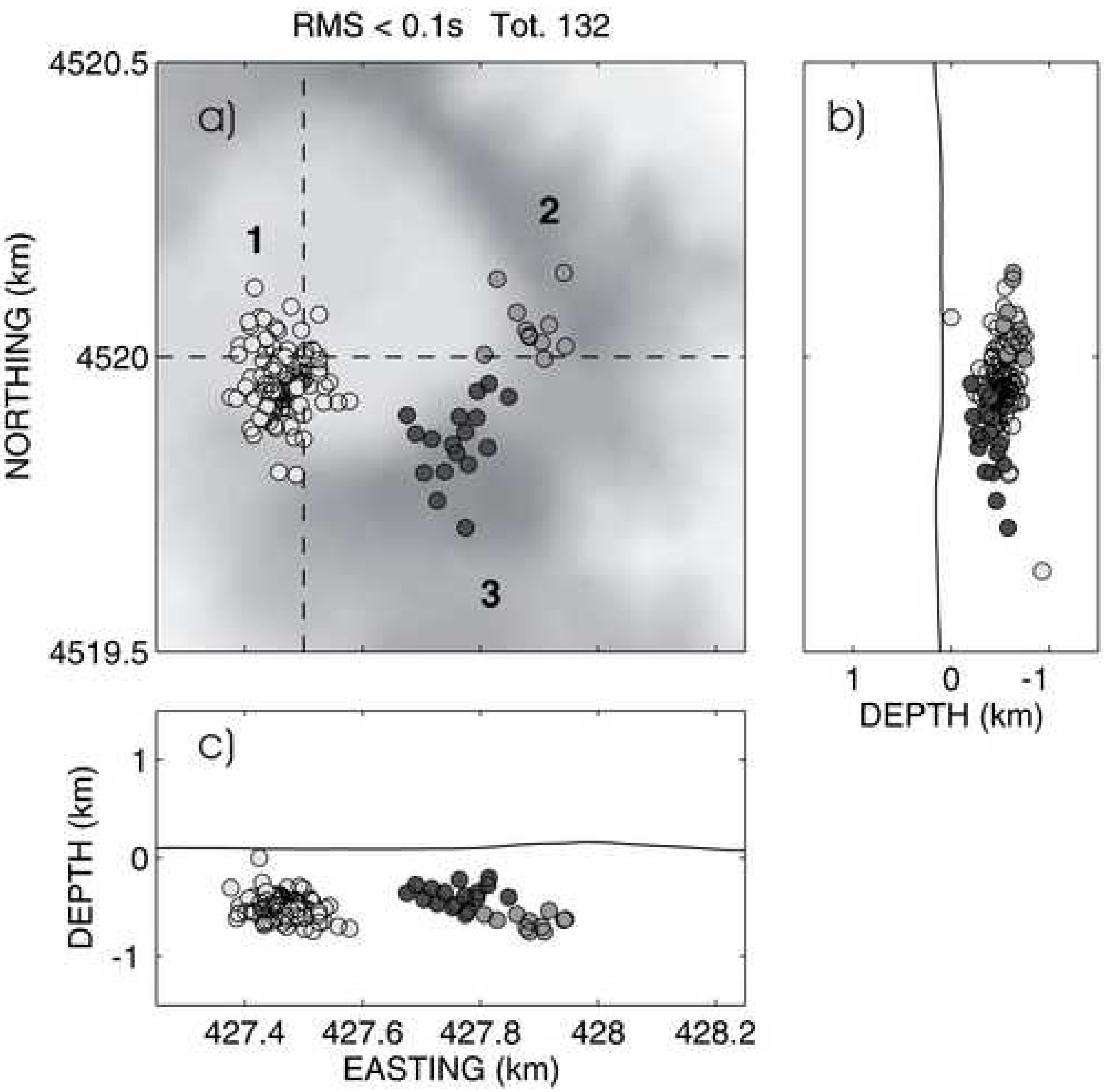
RMS < 0.1s Tot. 132
a)
b)
c)
1
2
3
4520.5
4520
4519.5
NORTHING (km)
1
0
-1
DEPTH (km)
DEPTH (km)
427.4
427.6
427.8
428
428.2
EASTING (km)

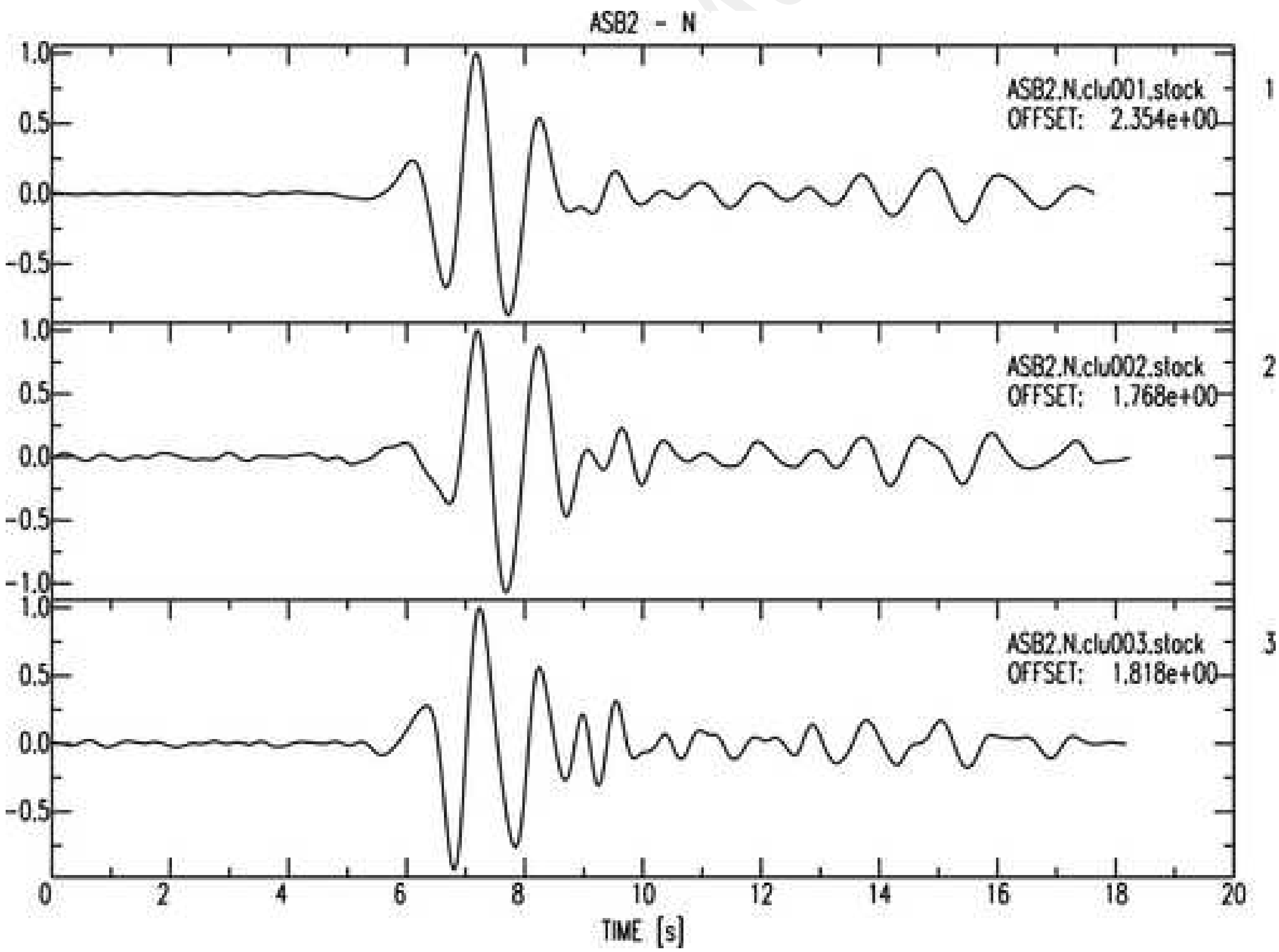
ASB2 - N
ASB2.N.clu001.stock
OFFSET: 2.354e+00
1
ASB2.N.clu002.stock
OFFSET: 1.768e+00
2
ASB2.N.clu003.stock
OFFSET: 1.818e+00
3
1.0
0.5
0.0
-0.5
-1.0
0
2
4
6
8
10
12
14
16
18
20
TIME [s]

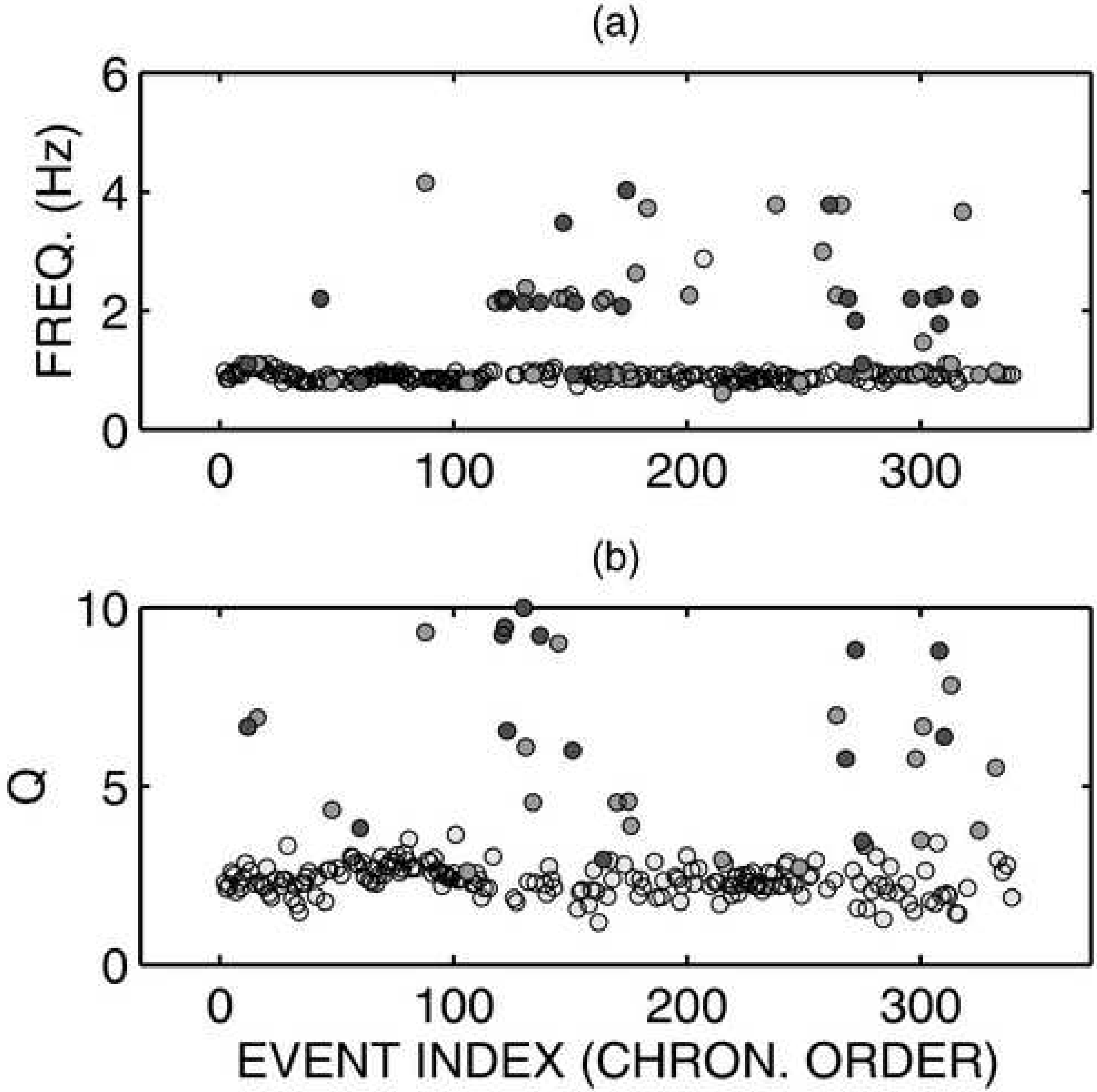
(a)
6
4
2
0
FREQ. (Hz)
0
100
200
300
(b)
10
5
0
Q
0
100
200
300
EVENT INDEX (CHRON. ORDER)

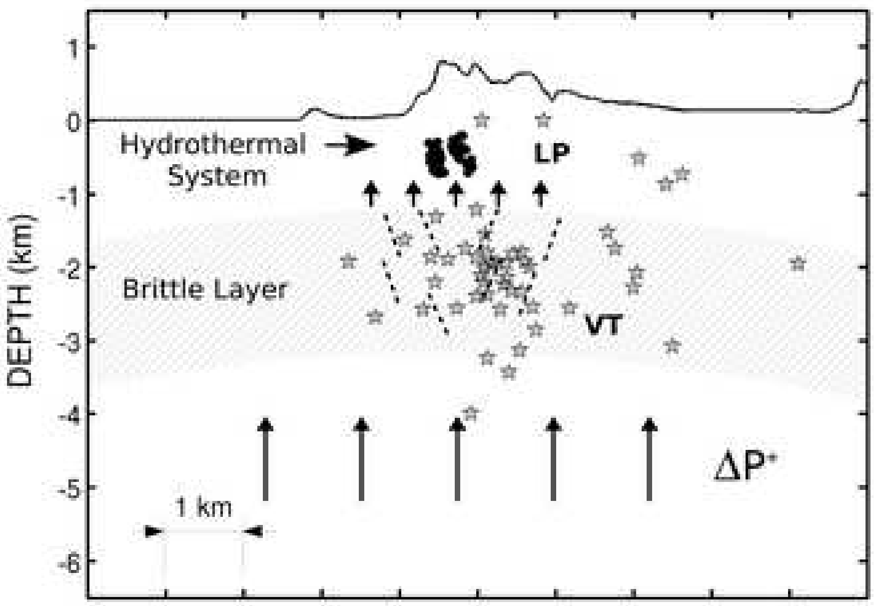
DEPTH (km)
1
0
-1
-2
-3
-4
-5
-6
Hydrothermal System
LP
Brittle Layer
VT
ΔP
1 km